nature genetics

© 2004 Nature Publishing Group http://www.nature.com/naturegenetics

ABCC9 mutations identified in human dilated cardiomyopathy disrupt catalytic K_{ATP} channel gating

Martin Bienengraeber[1,2], Timothy M Olson[1,3], Vitaliy A Selivanov[1], Eva C Kathmann[1,2], Fearghas O'Cochlain[1], Fan Gao[2], Amy B Karger[1,2], Jeffrey D Ballew[1], Denice M Hodgson[1], Leonid V Zingman[1,2], Yuan-Ping Pang[2], Alexey E Alekseev[1,2] & Andre Terzic[1,2]

Stress tolerance of the heart requires high-fidelity metabolic sensing by ATP-sensitive potassium (K_{ATP}) channels that adjust membrane potential–dependent functions to match cellular energetic demand. Scanning of genomic DNA from individuals with heart failure and rhythm disturbances due to idiopathic dilated cardiomyopathy identified two mutations in *ABCC9*, which encodes the regulatory SUR2A subunit of the cardiac K_{ATP} channel. These missense and frameshift mutations mapped to evolutionarily conserved domains adjacent to the catalytic ATPase pocket within SUR2A. Mutant SUR2A proteins showed aberrant redistribution of conformations in the intrinsic ATP hydrolytic cycle, translating into abnormal K_{ATP} channel phenotypes with compromised metabolic signal decoding. Defective catalysis-mediated pore regulation is thus a mechanism for channel dysfunction and susceptibility to dilated cardiomyopathy.

Cardiac K_{ATP} channels are heteromultimers composed of Kir6.2, an inwardly rectifying potassium channel pore, and the regulatory SUR2A subunit, an ATPase-harboring ATP-binding cassette protein[1–4]. The SUR2A subunit recognizes and processes intracellular energetic signals, through its nucleotide binding domains, endowing

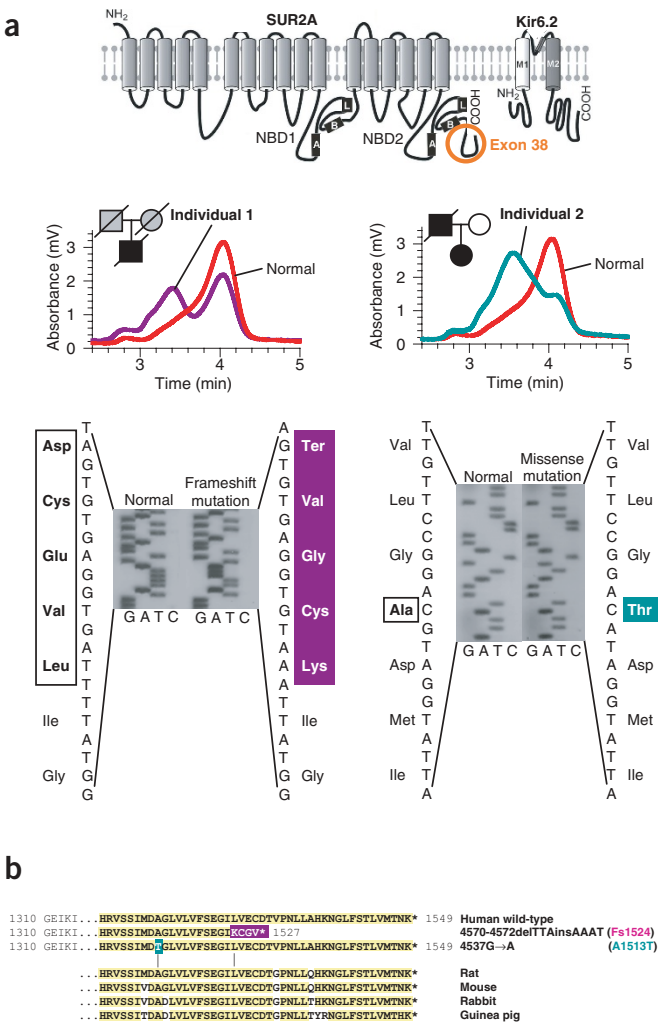

Figure 1 K_{ATP} channel mutations in dilated cardiomyopathy. (**a**) The regulatory SUR2A subunit (nucleotide-binding domains NBD1 and NBD2 with Walker A and B motifs and a linker L region) forms cardiac K_{ATP} channels by assembling with the pore-forming Kir6.2 subunit (transmembrane domains M1 and M2). Analysis of exon 38 in *ABCC9* genomic DNA, which encodes the C terminus of the SUR2A protein, identified abnormal chromatograms indicative of mutations in individuals with dilated cardiomyopathy (DCM). Sequencing identified frameshift (Fs1524; individual 1) and missense (A1513T; individual 2) mutations. The family of individual 1 was unavailable for segregation analysis. The mutation in individual 2 was not present in the proband's mother, suggestive of inheritance from the affected father (DNA was unavailable). (**b**) SUR2A residues encoded by exon 38 in wild-type and mutant *ABCC9* sequences in humans and other species.

[1]Division of Cardiovascular Diseases, Department of Medicine; [2]Department of Molecular Pharmacology and Experimental Therapeutics; and [3]Division of Pediatric Cardiology, Department of Pediatric and Adolescent Medicine, Mayo Clinic College of Medicine, Mayo Foundation, Rochester, Minnesota 55905, USA. Correspondence should be addressed to A.T. (terzic.andre@mayo.edu).

Published online 21 March 2004; doi:10.1038/ng1329

Table 1 Summary of clinical phenotypes

Individual	*ABCC9* mutation	Family history of DCM	Gender, age at diagnosis (y)	LVEDD (mm)[a]	EF (%)[b]	Coronary angiography	Cardiac rhythm[c]	Outcome
Individual 1	Frameshift (Fs1524)	No	Male, 55	65 (55)	23	Normal	Ventricular tachycardia	Death from heart failure at age 60 y
Individual 2	Missense (A1513T)	Yes	Female, 40	89 (52)	15	Normal	Ventricular tachycardia	Under intensive therapy
			Male, 54 Father of individual 2	81 (53)	13	Normal	Ventricular tachycardia	Death from heart failure at age 55 y

[a]LVEDD, left ventricular end-diastolic dimension. The 95th percentile values are given in parentheses. [b]EF, left ventricular ejection fraction. [c]Cardiac rhythm was documented by electrocardiographic monitoring.

© 2004 Nature Publishing Group http://www.nature.com/naturegenetics

the K_{ATP} channel-enzyme complex with a metabolic decoding capacity[5]. Potassium movement through Kir6.2 does not require energy expenditure[6], yet ATP hydrolysis at SUR2A is integral in the transduction of metabolic signals from cellular energetic pathways to the channel pore[5,7]. In this way, K_{ATP} channels set membrane excitability in response to stress challenge and preserve cellular energy-dependent functions[8–12]. Thereby, the K_{ATP} channel complex has a vital role in securing cellular homeostasis under stress[12].

Disease-induced K_{ATP} channel dysregulation, recently recognized in a transgenic model of cardiomyopathy, has been associated with compromised stress tolerance[13]. In fact, in the stressed heart, knockout of K_{ATP} channel genes precipitates intracellular calcium overload predisposing to myocardial damage, arrhythmia and death preventable by calcium-channel blockade[12]. Indeed, K_{ATP} channel–deficient hearts are susceptible to calcium-dependent maladaptive remodeling under chronic hemodynamic load, progressing to congestive heart failure (G.C. Kane, F.O., D.M.H., T. Miki, S. Seino and A.T., unpublished data). Although improper myocellular calcium handling contributes to the pathogenesis of dilated cardiomyopathy[14,15], a malignant disorder characterized by heart failure and increased susceptibility to metabolic stressors[16–18], little is known about K_{ATP} channels in human heart disease. Here, we report the first mutations in *ABCC9*, encoding SUR2A. Identified in individuals with idiopathic dilated cardiomyopathy, these defects in the regulatory K_{ATP} channel subunit disrupt catalysis-dependent gating and impair metabolic decoding, establishing a previously unrecognized mechanism of channel malfunction in human disease.

Scans for mutation in genomic DNA in a cohort of 323 individuals with idiopathic dilated cardiomyopathy identified two heterozygous mutations in exon 38 of *ABCC9*, which encodes the C-terminal domain of SUR2A specific to the cardiac splice variant of the regulatory K_{ATP} channel subunit (**Fig. 1a**,**b**). Both individuals with mutations in *ABCC9* had severely dilated hearts with compromised contractile function and rhythm disturbances (**Table 1**). DNA sequencing of one mutated allele identified a 3-bp deletion and 4-bp insertion mutation (4570-4572delTTAinsAAAT), causing a frameshift at Leu1524 and introducing four anomalous terminal residues followed by a premature stop codon (Fs1524; **Fig. 1a**). The second mutated allele harbored a missense mutation (4537G→A) causing the amino acid substitution A1513T (**Fig. 1a**). The identified frameshift and missense mutations occurred in evolutionarily conserved domains of the C terminus of SUR2A (**Fig. 1b**), and neither mutation was present in 500 unrelated control individuals.

The C terminus of SUR proteins contributes to K_{ATP} channel trafficking[19,20], and Fs1524 and A1513T SUR2A mutants, reconstituted with Kir6.2, had reduced expression in the plasma membrane (**Fig. 2a**). Yet, mutant K_{ATP} channel complexes formed functional channels with intact pore properties (**Fig. 2b**). Structural molecular dynamics simulation showed that the residues Ala1513 and Leu1524 flank the C-terminal β-strand in close proximity to the signature Walker A motif (**Fig. 2c**,**d**), required for coordination of nucleotides in the catalytic pocket of ATP-binding cassette proteins[21,22]. Replacement of Ala1513 with a sterically larger and more hydrophilic threonine residue or truncation of the C terminus caused by the Fs1524 mutation would

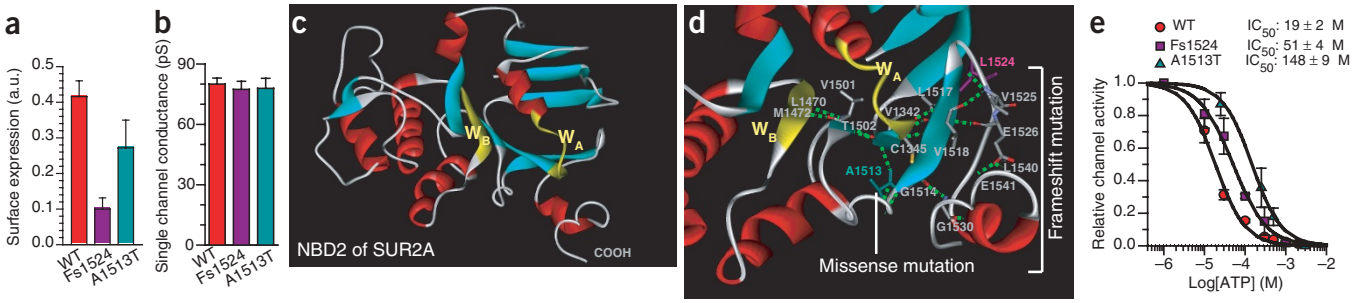

Figure 2 SUR2A mutant proteins, coexpressed with Kir6.2, alter K_{ATP} channel function. (**a**) Fs1524 and A1513T reduced K_{ATP} channel trafficking by ~70% and ~30%, probed immunologically by SUR surface expression in *Xenopus laevis* oocytes. (**b**) Single channel conductance and inward rectification (not shown) of wild-type and mutant channels, expressed in HEK293 cells, were identical, indicating that biophysical pore properties were intact. (**c**,**d**) Atomic model of SUR2A NBD2. Red, α-helix; blue, β-strand; yellow, Walker motifs (W_A and W_B). Missense A1513T (cyan) and frameshift L1524 (magenta) mutations frame the β-strand adjacent to Walker motifs that coordinate NBD2-mediated catalysis. Representative hydrogen bonds that stabilize Walker A and the associated C terminus β-strand are indicated by dashed green lines. Red, oxygen atoms; blue, nitrogen; mustard, sulfur (Cys1345). (**e**) Abnormal ATP-induced K_{ATP} channel inhibition in mutants. Channel inhibition was expressed relative to activity in the absence of ATP and measured at –60 mV in inside-out patches. Solid curves represent Hill equation fits of experimental data, with the ATP concentration required for half-inhibition (IC_{50}) indicated for wild-type and mutant channels.

disrupt folding of the C-terminal β-strand and, thus, the tertiary organization of the adjacent second nucleotide binding domain (NBD2) pocket in SUR2A. ATP-induced K_{ATP} channel gating was aberrant in both channel mutants (**Fig. 2e**), suggesting that structural alterations induced by the mutations A1513T and Fs1524 of SUR2A distorted ATP-dependent pore regulation.

On further examination, purified wild-type and mutant NBD2 constructs had similar ATP binding but reduced ATP hydrolytic activities (**Fig. 3a–c**). The A1513T and Fs1524 mutations substantially diminished the maximal rate of the NBD2 ATPase reaction without altering the Michaelis-Menten constant of catalysis (**Fig. 3d**). A1513T reduced the product-dependent inhibition of the NBD2 ATPase more substantially than Fs1524 (**Fig. 3e**) but produced a less severe delay in the pre–steady state profile of product accumulation (**Fig. 3f**). Thus, the mutations A1513T and Fs1524 compromise ATP hydrolysis at SUR2A NBD2, generating distinct reaction kinetic defects.

Aberrant catalytic properties in the A1513T and Fs1524 mutants translated into abnormal interconversion of discrete conformations in the NBD2 ATPase cycle (**Fig. 4a**). Each mutation doubled the rate constant of the SUR-ATP to SUR-ADP-P_i conversion (k_2), reducing the lifetime of SUR2A in the prehydrolytic state (**Fig. 4a**,**b**). Moreover, the rate constant of the SUR-ADP-P_i to SUR-ADP transition (k_3) was one hundred times lower in the Fs1524 mutant, markedly extending the lifetime of the SUR-ADP-P_i conformation and 'jamming' the ATPase cycle (**Fig. 4a–c**). Thus, in contrast to the catalytic reaction in the wild type, where the rate-limiting step is ADP dissociation (k_4), the Fs1524 ATPase is characterized by rate-limiting P_i dissociation (k_3; **Fig. 4c**). In contrast, the A1513T mutation delayed the ATPase cycle in the SUR-ADP conformation, by reducing the rate constant defining ADP dissociation (k_4) by a factor of 2, and reduced the ADP association rate constant (k_{04}) by a factor of 10 (**Fig. 4a–c**).

The ATPase cycle in both A1513T and Fs1524 mutants was abnormally delayed in a posthydrolytic conformation, SUR-ADP-P_i or SUR-ADP. Although they had distinct patterns of lifetime distribution, each mutation diminished the likelihood that SUR2A could adopt a prehydrolytic conformation and increased the probability of posthydrolytic conformations (**Fig. 4d**). Individual conformations of the SUR2A ATPase cycle have distinct impacts on K_{ATP} channel regulation, with the prehydrolytic SUR-ATP state promoting channel closure and the posthydrolytic SUR-ADP-P_i and SUR-ADP states favoring channel activation[5]. Consequently, alterations in hydrolysis-driven SUR2A conformational probability induced by A1513T and Fs1524 translated into abnormal ATP sensitivity of mutant channels (**Fig. 2e**).

Under metabolic stress, the increase in intracellular ADP favors posthydrolytic ADP-bound conformations associated with antagonism of ATP-induced K_{ATP} channel pore inhibition[5,10]. ADP-dependent K_{ATP} channel regulation, and thus the channel's stress responsiveness, are represented by the relative shift from prehydrolytic to posthydrolytic of the conformational probability (P) of the ATPase induced by changes in ADP (dP/d[ADP]). Compared to the wild type and at any given ATP level, A1513T and Fs1524 mutants were less responsive in ADP-induced redistribution of post- (**Fig. 4e**) and prehydrolytic (**Fig. 4f**) conformations. Accordingly, metabolic pathways, like the creatine kinase phosphotransfer system[23], effectively regulated ATPase activity of wild-type but not mutant SUR2A (**Fig. 4g**). In fact, aberrant catalysis in mutant SUR2A generated defective K_{ATP} channel phenotypes characterized by abnormal responses to both ATP (**Fig. 2e**) and ADP (**Fig. 4h**,**i**), mediators of the cellular energetic state. Thus, the mutations A1513T and

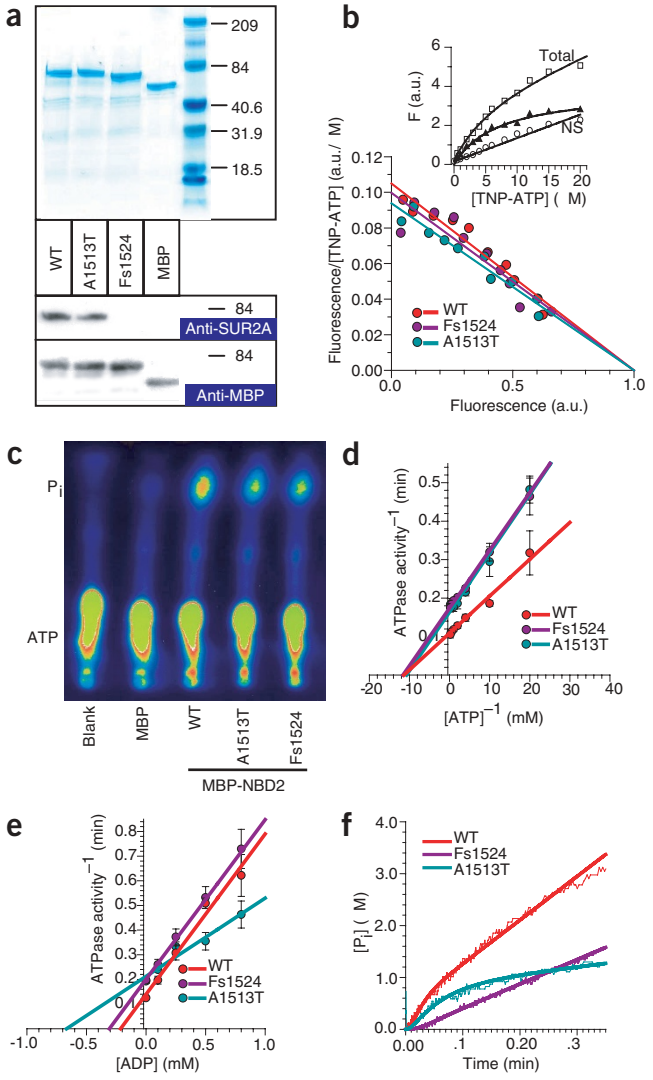

Figure 3 SUR2A NBD2 mutants have normal ATP binding but altered ATPase properties. (**a**) Affinity-purified mutant or wild-type SUR2A NBD2, cloned in-frame with maltose binding protein (MBP), on SDS gels. An antibody against the last 12 amino acids of SUR2A recognized the wild-type (WT) and A1513T mutant but not Fs1524, whereas an antibody raised against MBP reacted with all constructs. Molecular sizes are given in kDa. (**b**) The binding affinity of the fluorescent ATP analog TNP-ATP was similar for wild-type (WT) and mutant NBD2 in Scatchard analysis. Inset: Specific TNP-ATP binding-induced signal detected as difference between total and nonspecific (NS) fluorescence (F) of the ATP analog in the absence of NBD constructs. (**c**) The A1513T and Fs1524 NBD2 mutations reduced ATPase activity measured from γ-^{32}P liberation after [γ-^{32}P]ATP hydrolysis. WT, wild-type. (**d**,**e**) ATP and ADP dependence of NBD2 ATPase activities measured by spectrophotometry showed v_{max} values of 9.98 ± 0.34 min^{-1} in wild-type (WT), 6.07 ± 0.18 min^{-1} in A1513T and 5.69 ± 0.29 min^{-1} in Fs1524 with Michaelis-Menten constants at 0.11 ± 0.02, 0.094 ± 0.013 and 0.084 ± 0.010 mM, respectively (equation 3). The ATP-dependence of the NBD2 ATPase was determined at 0 ADP in the presence of creatine kinase (0.01 U ml^{-1}) and creatine phosphate (5 mM). ADP-dependent inhibition of the NBD2 ATPase (at 2 mM ATP) was characterized by an ADP-dissociation constant (K_{ADP}) of 8.6 ± 0.3 M in wild-type versus 24.9 ± 5.6 and 11.0 ± 1.5 in the A1513T and Fs1524 mutants, respectively (equation 5). (**f**) Both pre–steady state and steady-state reaction rates were altered by A1513T and Fs1524 mutations in stopped-flow experiments. Solid lines represent the fit of experimental data with the system of differential equations (equation 6), allowing evaluation of the rate kinetic constants of the NBD2 ATPase reaction. WT, wild-type.

© 2004 Nature Publishing Group http://www.nature.com/naturegenetics

© 2004 Nature Publishing Group http://www.nature.com/naturegenetics

Fs1524 altered intrinsic catalytic properties of the SUR2A ATPase, compromising proper translation of cellular energetic signals into K_{ATP} channel-mediated membrane electrical events.

K_{ATP} channel mutations, identified here in two individuals with dilated cardiomyopathy, underscore the essential role of the intrinsic enzymatic reaction in cardiac channel pore regulation. Aberrant kinetics of hydrolysis at the regulatory channel subunit, despite unaltered nucleotide binding, produced defective metabolic signal decoding. Thus, nucleotide-dependent regulation of the stress-responsive K_{ATP} channel is based not only on conventional competition between ATP and ADP at nucleotide binding domains[24] but also on the profile of conformational interconversion driven by the catalytic cycle in the regulatory channel subunit. Traditionally linked to defects in ligand interaction, subunit trafficking or pore conductance[10,20,25], human cardiac K_{ATP} channel dysfunction provoked by alterations in the catalytic module of the channel complex establishes a new mechanism for channelopathy. In this way, defective ion channel function would confer susceptibility to dilated cardiomyopathy.

METHODS

Mutational analysis. We carried out mutation scans of K_{ATP} channel genes in individuals, predominantly of European descent, with idiopathic dilated cardiomyopathy who gave informed consent with approval from the Mayo Clinic Institutional Review Board. According to established diagnostic criteria, individuals had left ventricular dimensions >95th percentile indexed for body surface area and age and left ventricular ejection fractions <50% as determined by echocardiography. We designed primers for exon-specific PCR amplification using the OLIGO v6.51 Primer Analysis Software (National Biosciences) and the WAVEMAKER version 4.0.32 Software (Transgenomic). We identified sequence variants in PCR-amplified DNA fragments by denaturing high-performance liquid chromatography heteroduplex analysis (WAVE DNA Fragment Analysis System, Transgenomic). We amplified fragments that formed heteroduplexes by PCR and cycle-sequenced them using a Thermo Sequenase kit (Amersham Life Sciences). To confirm mutations, we isolated mutated alleles on 1X Mutation Detection Enhancement gels (FMC Bioproducts), reamplified them and sequenced them[26]. Healthy blood donors served as controls.

Homology modeling and molecular dynamics simulation. We generated the three-dimensional model of SUR2A NBD2 using the homology modeling program MODELLER 6 using as a template the crystal structure of the ATPase domain in the human TAP1 protein with ADP in the binding pocket (PDB code 1JJ7) identified by the FASTA search[27]. We refined the initial atomic NBD2 three-dimensional model by energy minimizations and a 2.0-ns (1.0-fs time step) molecular dynamics simulation using the AMBER 5.0/6.0 program with a second generation force field (parm96.dat) according to established protocols[28].

Cloning of K_{ATP} channel subunits and purification of SUR2A ATPase. We subcloned cDNAs encoding SUR2A and Kir6.2 cDNA into the expression vector pcDNA3.1. We carried out PCR-based site-directed mutagenesis using

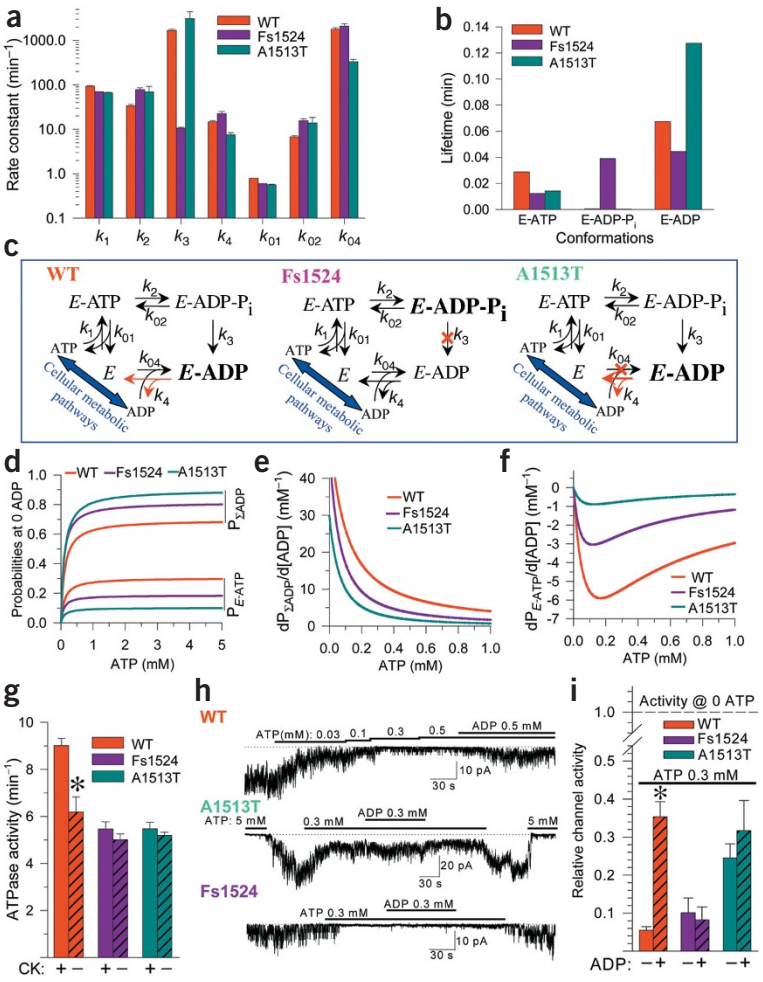

Figure 4 Altered kinetics of the ATPase cycle lead to disrupted metabolic decoding by K_{ATP} channels. (**a**) Rate constants defining the SUR2A ATPase reaction were derived from pre–steady state kinetics of P_i liberation in wild-type (WT) and mutant NBD2 constructs ($n = 4$ each). (**b**) Lifetime distribution of individual conformations (equation 10) in wild-type (WT) and mutant NBD2 ATPase cycle. (**c**) Rate-limiting steps in the SUR2A ATPase cycle are ADP dissociation (k_4) for wild-type (WT), P_i dissociation (k_3) for Fs1524 and abnormally increased k_4 for A1513T. Fs1524 has the lowest k_{04} rate constant defining ADP association. (**d**) In the absence of ADP, both NBD2 mutants have lower probability to adopt ATP-bound ($P_{E\text{-}ATP}$) and higher probability to adopt ADP-bound ($P_{\Sigma ADP}$) conformations in a wide range of ATP concentrations. $P_{\Sigma ADP}$ is the sum of *E*-ADP-P_i ($P_{E\text{-}ADP\text{-}Pi}$) and *E*-ADP ($P_{E\text{-}ADP}$) probabilities (equations 7–9). WT, wild-type. (**e**,**f**) ADP-induced modulation of probabilities in the NBD2 ATPase cycle intermediates determined as $dP_{\Sigma ADP}/d[ADP]$ and $dP_{E\text{-}ATP}/d[ADP]$ derivatives at different ATP levels. In response to ADP, $P_{\Sigma ADP}$ increases whereas $P_{E\text{-}ATP}$ decreases, defining the sign of respective derivatives. Both Fs1524 and A1513T diminished the ADP-responsiveness of $P_{\Sigma ADP}$ and $P_{E\text{-}ATP}$. WT, wild-type. (**g**) ADP-scavenging creatine kinase (0.01 U ml^{-1}, 5 mM creatine phosphate) accelerates the ATPase in the wild type (WT) but not in Fs1524 and A1513T mutants. Rate of P_i liberation was measured at 2 mM ATP using spectrophotometry. (**h**,**i**) After coexpression of Kir6.2, channel activity, at 0.3 mM ATP, in the presence and absence of 0.3 mM ADP was measured in wild-type (WT; $n = 5$) SUR2A and in Fs1524 ($n = 4$) and A1513T ($n = 6$) SUR2A mutants in inside-out patches. In addition to reduced ATP sensitivity, both mutants had blunted ADP channel response relative to K_{ATP} channel activity at zero nucleotide levels.

© 2004 Nature Publishing Group http://www.nature.com/naturegenetics

primers incorporating identified mutations (QuickChange, Stratagene). We sequenced the constructs to verify mutations and rule out additional changes in sequence. We purified soluble SUR2A NBD2 (Thr1220–Thr1546) by overexpressing a fusion protein construct containing the maltose binding protein (MBP) used for affinity chromatography on an amylose resin in 600 mM NaCl, 1 mM EDTA, 20 mM Tris, 1 mM dithiothreitol and 10% glycerol[3,5,7].

Enzymology and nucleotide binding. We measured ATPase activity of purified NBD2, in the presence of Mg^{2+}, as P_i generation detected spectrophotometrically at 360 nm with the EnzChek Phosphate Assay Kit or by monitoring conversion of [γ-^{32}P]ATP using thin layer chromatography and quantified it with PhosphorImager and ImageQuant software (Molecular Dynamics)[3,5,7]. We captured the initial kinetics of ATP hydrolysis by stopped-flow spectroscopy with instantaneous mixing of purified protein and substrate on an SX.18MV spectrometer (Applied Photophysics). We determined binding of fluorescent ATP analog TNP-ATP to purified NBD2 constructs by fluorescence spectrophotometry (QuantaMaster, PTI) at excitation and emission wavelengths of 410 nm and 540 nm, respectively.

Surface channel subunit expression. We injected cRNA encoding wild-type or mutant SUR2A (6 ng), tagged with an extracellular hemagglutinin epitope, with cRNA encoding Kir6.2 (2 ng) into *Xenopus laevis* oocytes[29]. After 72 h, we labeled oocytes at 4 °C with 0.4 g ml^{-1} monoclonal antibody to hemagglutinin and horseradish peroxidase–coupled secondary antibody. Chemiluminescence at the plasmalemma of individual oocytes, generated from channel proteins that trafficked to the surface, was captured in Power Signal ELISA solution (Pierce) and quantified using a plate reader (Lab Systems).

Electrophysiology. We cotransfected human embryonic kidney (HEK293) cells, cultured at 5% CO_2 in Dulbecco's modified Eagle medium with 10% fetal calf serum and 2 mM glutamine, with 0.5 g of reporter green fluorescent protein and 6 g of total plasmid DNA (cDNAs encoding wild-type or mutant SUR2A and Kir6.2 at a 5:1 ratio) using 15 l of Fugene (Roche). We applied the patch-clamp technique using patch electrodes filled with 140 mM KCl, 1 mM $CaCl_2$, 1 mM $MgCl_2$ and 5 mM HEPES buffer (pH 7.3) and superfused the cells with 140 mM KCl, 1 mM $MgCl_2$, 5 mM EGTA and 5 mM HEPES-KOH buffer (pH 7.3). We measured K_{ATP} channel activity at 31 ± 1 °C using a temperature controller (HCC-100A; Dagan)[5].

Kinetics of SUR2A ATPase. In the ATPase catalytic cycle,

$$E + \mathrm{ATP} \underset{k_{01}}{\overset{k_1}{\leftrightarrow}} E^{*} - \mathrm{ATP} \underset{k_{02}}{\overset{k_2}{\leftrightarrow}} E^{**} - \mathrm{ADP} - \mathrm{P_i} \overset{k_3}{\rightarrow} E^{***} - \mathrm{ADP} + \mathrm{P_i} \underset{k_{04}}{\overset{k_4}{\leftrightarrow}} E + \mathrm{ADP} + \mathrm{P_i},$$

E is SUR2A and stars indicate distinct conformations during Mg^{2+}-dependent ATP hydrolysis. Transitions are bidirectional, with the exception of the P_i liberation step (k_3), which is irreversible in SUR2A NBD2 constructs. Therefore, the steady-state rate equation of the ATPase reaction was derived by the King-Altman method:

$$(1)\quad \frac{E_t}{v} = \frac{slope_1}{[\mathrm{ATP}]} + \frac{[\mathrm{ADP}]slope_1}{[\mathrm{ATP}]K_{\mathrm{ADP}}} + \frac{1}{v_{\max}}$$

and

$$(2)\quad slope_1 = \frac{1}{k_1} + \frac{K_{\mathrm{ATP}}}{k_2} + \frac{K_{\mathrm{ATP}}}{k_3 K_{\mathrm{ADP\text{-}P_i}}} \text{ and } \frac{1}{v_{\max}} = \frac{1}{k_2} + \frac{1}{k_3} + \frac{1}{k_3 K_{\mathrm{ADP\text{-}P_i}}} + \frac{1}{k_4}$$

where E_t is total enzyme amount, v is the reaction rate, $slope_1$ is the slope of double-reciprocal dependence of the reaction rate v on ATP (at [ADP] = 0), v_{max} is the maximal reaction rate, $K_{ATP} = k_{-1}/k_1$, $K_{ADP\text{-}Pi} = k_2/k_{-2}$ and $K_{ADP} = k_4/k_{-4}$.

We determined the ADP dissociation constant, K_{ADP}, from spectrometric measurement of steady-state NBD2 ATPase activity at [ADP] = 0 with variable [ATP]. Equation 1 can thus be simplified:

$$(3)\quad E_t/v = slope_1/[\mathrm{ATP}] + 1/v_{\max},$$

where $slope_1$ and v_{max} are assessable for experimental determination. At variable [ADP], with constant [ATP] ([ATP]$_c$), equation 1 is a linear function of [ADP]:

$$(4)\quad E_t/v = [\mathrm{ADP}]slope_1/K_{\mathrm{ADP}}[\mathrm{ATP}]_c + slope_1/[\mathrm{ATP}]_c + 1/v_{\max},$$

where the slope of the reciprocal reaction rate $slope_2 = slope_1/K_{ADP}[ATP]_c$. Thus, K_{ADP} was defined:

$$(5)\quad K_{\mathrm{ADP}} = slope_1/slope_2[\mathrm{ATP}].$$

We defined kinetic rate constants of the ATPase reaction using stopped-flow spectroscopy where virtually instantaneous initiation of the ATPase reaction was achieved by mixture of NBD2 constructs and MgATP (2 mM ATP, 3 mM $MgCl_2$). During the first catalytic cycle, the time required to reach the step of P_i liberation is shorter than in subsequent reaction cycles. Therefore, the rate of reaction product accumulation in the initial pre–steady state is higher than in the following steady-state reaction. Kinetic parameters of the ATPase cycle were defined by fitting the kinetics of product accumulation with a system of differential equations with equations 2 and 5:

$$(6)\quad d[E]/dt = -[E](k_1[\mathrm{ATP}] + k_{-4}[\mathrm{ADP}]) + [E\text{-ATP}]k_{-1} + (E_t - [E] - [E\text{-ATP}] - [E\text{-ATP-P}_i]k_4$$
$$d[E\text{-ATP}]/dt = [E]k_1[\mathrm{ATP}] - [E\text{-ATP}](k_{-1} + k_2) + [E\text{-ATP-P}_i]\,k_{-2}$$
$$d[E\text{-ADP-P}_i]/dt = -[E\text{-ADP-P}_i](k_{-2} + k_3) + [E\text{-ATP}]k_2$$
$$d[P_i]/dt = [E\text{-ATP-Pi}]k_3$$
$$d[E\text{-ADP}]/dt = (E_t - [E] - [E\text{-ATP}] - [E\text{-ATP-P}_i])k_4 + [E][\mathrm{ADP}]k_{-4},$$

where E_t is the total enzyme amount. We solved the system using the Runge-Kutta algorithm. We calculated probabilities for NBD2 ATPase conformations (*E*-ATP, *E*-ADP-P_i and *E*-ADP) as:

$$(7)\quad P_{E\text{-ATP}} = D_{E\text{-ATP}}/(D_E + D_{E\text{-ATP}} + D_{E\text{-ADP-P}_i} + D_{E\text{-ADP}}),$$

$$(8)\quad P_{E\text{-ADP-P}_i} = D_{E\text{-ADP-P}_i}/(D_E + D_{E\text{-ATP}} + D_{E\text{-ADP-P}_i} + D_{E\text{-ADP}}) \text{ and}$$

$$(9)\quad P_{E\text{-ADP}} = D_{E\text{-ADP}}/(D_E + D_{E\text{-ATP}} + D_{E\text{-ADP-P}_i} + D_{E\text{-ADP}}),$$

where $D_E = (k_2k_3 + k_{-1}k_3 + k_{-1}k_{-2})k_4$; $D_{E\text{-ATP}} = (k_3 + k_{-2})k_1k_4[\mathrm{ATP}]$; $D_{E\text{-ADP-Pi}} = k_1k_2k_4[\mathrm{ATP}]$; and $D_{E\text{-ADP}} = k_1k_2k_3[\mathrm{ATP}] + (k_2k_3 + k_{-1}k_3 + k_{-1}k_{-2})k_{-4}[\mathrm{ADP}]$.

We defined lifetimes of conformations in the ATPase cycle as reciprocal values of the sum of rates leading away from particular conformations:

$$(10)\quad \tau_{E\text{-ATP}} = 1/(k_{-1} + k_2);\ \tau_{E\text{-ADP-P}_i} = 1/(k_{-2} + k_3);\ \tau_{E\text{-ADP}} = 1/k_4,\ (k_{-3} = 0).$$

ACKNOWLEDGMENTS

We thank J. Bryan, Y. Kurachi and S. Seino for K_{ATP} channel clones; B. Schwappach for constructs used in trafficking studies; and T.P. Burghardt and A.J. Caride for technical advice. This work was supported by the US National Institutes of Health, American Heart Association, Miami Heart Research Institute, Marriott Foundation, Siragusa Foundation, University of Minnesota Supercomputing Institute, Mayo-Dubai Healthcare City Research Project and Mayo Foundation. A.T. is an Established Investigator of the American Heart Association.

COMPETING INTERESTS STATEMENT

The authors declare that they have no competing financial interests.

Received 29 November 2003; accepted 13 February 2004
Published online at http://www.nature.com/naturegenetics/

1. Inagaki, N. *et al.* Reconstitution of IK_{ATP}: An inward rectifier subunit plus the sulfonylurea receptor. *Science* **270**, 1166–1170 (1995).
2. Inagaki, N. *et al.* A family of sulfonylurea receptors determines the pharmacological properties of ATP-sensitive K^+ channels. *Neuron* **16**, 1011–1017 (1996).
3. Bienengraeber, M. *et al.* ATPase activity of the sulfonylurea receptor: A catalytic function for the K_{ATP} channel complex. *FASEB J.* **14**, 1943–1952 (2000).
4. Matsuo, M., Tanabe, K., Kioka, N., Amachi, T. & Ueda, K. Different binding properties and affinities for ATP and ADP among sulfonylurea receptor subtypes, SUR1, SUR2A, and SUR2B. *J. Biol. Chem.* **275**, 28757–28763 (2000).
5. Zingman, L.V. *et al.* Signaling in channel/enzyme multimers: ATPase transitions in

SUR module gate ATP-sensitive K^+ conductance. *Neuron* **31**, 233–245 (2001).
6. Tucker, S.J., Gribble, F., Zhao, C., Trapp, S. & Ashcroft, F.M. Truncation of Kir6.2 produces ATP-sensitive K^+ channels in the absence of the sulphonylurea receptor. *Nature* **387**, 179–183 (1997).
7. Zingman, L.V. *et al.* Tandem function of nucleotide binding domains confers competence to sulfonylurea receptor in gating ATP-sensitive K^+ channels. *J. Biol. Chem.* **277**, 14206–14210 (2002).
8. Weiss, J.N. & Lamp, S.T. Glycolysis preferentially inhibits ATP-sensitive K^+ channels in isolated guinea pig cardiac myocytes. *Science* **238**, 67–69 (1987).
9. O'Rourke, B., Ramza, B. & Marban, E. Oscillations of membrane current and excitability driven by metabolic oscillations in heart cells. *Science* **265**, 962–966 (1994).
10. Nichols, C.G. *et al.* Adenosine diphosphate as an intracellular regulator of insulin secretion. *Science* **272**, 1785–1787 (1996).
11. Yamada, K. *et al.* Protective role of ATP-sensitive potassium channels in hypoxia-induced generalized seizure. *Science* **292**, 1543–1546 (2001).
12. Zingman, L.V. *et al.* Kir6.2 is required for adaptation to stress. *Proc. Natl. Acad. Sci. USA* **99**, 13278–13283 (2002).
13. Hodgson, D.M. *et al.* Cellular remodeling in heart failure disrupts K_{ATP} channel-dependent stress tolerance. *EMBO J.* **22**, 1532–1542 (2003).
14. Schmitt, J.P. *et al.* Dilated cardiomyopathy and heart failure caused by a mutation in phospholamban. *Science* **299**, 1410–1413 (2003).
15. Chien, K.R., Ross, J. & Hoshijima, M. Calcium and heart failure. *Nat. Med.* **9**, 508–509 (2003).
16. Chien, K.R. Stress pathways and heart failure. *Cell* **98**, 555–558 (1999).
17. Seidman, J.G. & Seidman, C. The genetic basis for cardiomyopathy: From mutation identification to mechanistic paradigms. *Cell* **104**, 557–567 (2001).
18. Towbin, J.A. & Bowles, N.E. The failing heart. *Nature* **415**, 227–233 (2002).
19. Sharma, N. *et al.* The C terminus of SUR1 is required for trafficking of K_{ATP} channels. *J. Biol. Chem.* **274**, 20628–20632 (1999).
20. Cartier, E.A., Conti, L.R., Vandenberg, C.A. & Shyng, S.L. Defective trafficking and function of K_{ATP} channels caused by a sulfonylurea receptor 1 mutation associated with persistent hyperinsulinemic hypoglycemia of infancy. *Proc. Natl. Acad. Sci. USA* **98**, 2882–2887 (2001).
21. Walker, J.E., Saraste, M., Runswick, M. & Gay, N. Distantly related sequences in the alpha- and beta-subunits of ATP synthase, myosin, kinases and other ATP-requiring enzymes and a common nucleotide binding fold. *EMBO J.* **1**, 945–951 (1982).
22. Matsushita, K. *et al.* Intramolecular interaction of SUR2 subtypes for intracellular ADP-induced differential control of K_{ATP} channels. *Circ. Res.* **90**, 554–561 (2002).
23. Abraham, M.R. *et al.* Coupling of cell energetics with membrane metabolic sensing. Integrative signaling through creatine kinase phosphotransfer disrupted by M-CK gene knock-out. *J. Biol. Chem.* **277**, 24427–24434 (2002).
24. Noma, A. ATP-regulated K^+ channels in cardiac muscle. *Nature* **305**, 147–148 (1983).
25. Nestorowicz, A. *et al.* A nonsense mutation in the inward rectifier potassium channel gene, Kir6.2, is associated with familial hyperinsulinism. *Diabetes* **46**, 1743–1748 (1997).
26. Olson, T.M. *et al.* Actin mutations in dilated cardiomyopathy, a heritable form of heart failure. *Science* **280**, 750–752 (1998).
27. Gaudet, R. & Wiley, D.C. Structure of the ABC ATPase domain of human TAP1, the transporter associated with antigen processing. *EMBO J.* **20**, 4964–4972 (2001).
28. Pang, Y.P. Successful molecular dynamics simulation of two zinc complexes bridged by a hydroxide in phosphotriesterase using the cationic dummy atom method. *Proteins* **45**, 183–189 (2001).
29. Schwappach, B., Zerangue, N., Jan, Y.N. & Jan, L.Y. Molecular basis for K_{ATP} assembly: transmembrane interactions mediate association of a K^+ channel with an ABC transporter. *Neuron* **26**, 155–167 (2000).

© 2004 Nature Publishing Group http://www.nature.com/naturegenetics